Energy Reports 8 (2022) 7945–7956

Contents lists available at ScienceDirect

Energy Reports

journal homepage: www.elsevier.com/locate/egyr

Research paper

Experimental study of a sustainable cooling process hybridizing indirect evaporative cooling and mechanical vapor compression

Qian Chen [a,*], M. Kum Ja [a], Muhammad Burhan [a], Muhammad Wakil Shahzad [a,b], Doskhan Ybyraiymkul [a], Hongfei Zheng [c], Kim Choon Ng [a]

[a] Water Desalination and Reuse Center, Biological and Environmental Science and Engineering Division, King Abdullah University of Science and Technology, Thuwal 23955, Saudi Arabia
[b] Northumbria University, Newcastle Upon Tyne, United Kingdom
[c] School of Mechanical Engineering, Beijing Institute of Technology, Beijing 100081, China

ARTICLE INFO

Article history:
Received 20 March 2022
Received in revised form 15 May 2022
Accepted 15 June 2022
Available online xxxx

Keywords:
Indirect evaporative cooling
Mechanical vapor compression
Hybrid cooling system
Experimental study
Rapid evaluation model

ABSTRACT

The hybrid indirect evaporative cooling-mechanical vapor compression (IEC-MVC) process is an emerging cooling technology that combines the advantages of IEC and MVC, i.e., effective temperature and humidity control, high energy efficiency, and low water consumption. This paper presents an experimental study of the hybrid IEC-MVC process. A 1-Rton pilot is fabricated by connecting IEC and MVC in series, and its performance is evaluated under different operating conditions (outdoor air temperature and humidity, air flowrate, compressor frequency). Results revealed that the outdoor air temperature and humidity could be lowered to 5–15 °C and 5–10 g/kg, respectively. The IEC handles 35%–50% of the total cooling load, and the energy consumption can be reduced by 15%–35% as compared to standalone MVC. Moreover, the condensate collected from the evaporator can compensate for >70% of water consumption in IEC, making the system applicable in arid regions. Based on the derived results, a simplified empirical model is developed for rapid evaluation of the IEC-MVC process, and the energy-saving potential in major cities of Saudi Arabia is estimated.

1. Introduction

With the growth of the global population and increase of living standards, the demand for air-conditioning (AC) has been increasing rapidly in the past few decades. It is projected that the global AC stock will reach 5000 million units by 2050, and the corresponding electricity consumption will exceed 6000 TWh (IEA, 2021). Therefore, reducing the energy consumption for AC is one of the most critical ways to alleviate global energy stress and cut CO_2 emissions.

The Gulf Cooperation Council (GCC) region is among the areas that have the highest cooling demands. The annual cooling load in GCC countries exceeds 36 million Rton (Eveloy and Ayou, 2019), and the energy consumption of AC accounts for 50%–70% of peak electricity demand (Eveloy and Ayou, 2019). The required cooling is mainly provided by mechanical vapor compression (MVC) chillers due to their high technical maturity and low costs. However, MVC suffers from a low energy efficiency in this region due to the high ambient temperature and poor air quality (Shahzad et al., 2019, 2021). In order to reduce the primary energy consumption, the industry has been searching for more sustainable alternatives to MVC chillers.

The indirect evaporative cooler (IEC) is deemed a promising technology for cooling applications. It utilizes the evaporation of water as the driving force for cooling. As the evaporation heat of water (>2200 kJ/kg) is much higher than the heat capacity of air (~1 kJ/kg-°C), substantial cooling effects can be produced by evaporating a small amount of water. The only power input in this process is the electricity consumption of the fans and the water pumps, which is insignificant compared to the cooling power. As a result, the energy efficiency of IEC is several times higher than MVC (Jradi and Riffat, 2014).

Extensive research efforts have been reported to improve IEC's performance, and the latest ones can be categorized into the following: (i) proposing novel configurations for IEC heat and mass exchanger, (ii) enhancing heat and mass transfer in dry and wet channels, and (iii) exploring new materials for system fabrication. Conventional IECs are flat-plate heat exchangers with cross-flow or counter-flow configurations (Min et al., 2019a; Yang et al., 2021). The Maisotsenko-cycle (M-cycle) cooler (Baakeem et al., 2019; Oh et al., 2019) and the regenerative indirect evaporative cooler (RIEC) (Cui et al., 2019a; Duan et al., 2016) are two prominent examples, which can cool the air to below its wet-bulb temperature. Compared with cross-flow, the counter-flow

* Corresponding author.
E-mail address: chen_qian@u.nus.edu (Q. Chen).

https://doi.org/10.1016/j.egyr.2022.06.019

configuration is more complex but demonstrates better performance. For an optimal trade-off between complexity and cooling performance, the counter-cross-flow configuration was recently proposed (Jia et al., 2019; Pandelidis et al., 2020). Its fabrication is simple like cross-flow IEC, while the cooling performance is close to that of counter-flow IEC. Other novel configurations include the tubular IEC and the heat-pipe IEC. The former has a more uniform water distribution (Wang et al., 2017; Duan et al., 2012), and the latter enhances heat and mass transfer between dry and wet channels (Boukhanouf et al., 2018; Riffat and Zhu, 2004).

Research efforts have also been reported to enhance heat and mass transfer inside IEC by adding internal structures, e.g., corrugated wick structures, baffles, and fins. Corrugated wick structures made from cotton or paper can not only increase the heat and mass transfer area but also improve wettability (Park et al., 2019). Moshari and Heidarinejad (2017) added wick materials in the wet channels of IEC and observed better evaporative cooling effects, but the pressure drop of air was also higher. Kabeel et al. (2017) and Kabeel and Abdelgaied (2016) introduced baffles in the dry channels, which created internal vortexes and increased the wet-bulb effectiveness by >33%. Ali et al. (2021) added aluminum fins in the dry channels and enhanced the cooling capacity by 18%.

The effects of material selection on IEC have also been explored. Aluminum is the most widely used material because of its good thermal conductivity and hydrophilicity (Yang et al., 2021). Moreover, the aluminum plate is thin and has negligible thermal resistance (Zhao et al., 2008). Porous ceramics are another promising option due to their high porosity, good thermal conductivity, and high corrosion resistance (Rashidi et al., 2019). Wang et al. (2017) demonstrated that the tubular ceramic IEC could maintain the cooling capacity for 100 min after 5 min of water spray. Boukhanouf et al. (2017) presented a plate-type IEC made of a ceramic water container. The maximum cooling capacity was 225 W/m^2, and the wet-bulb effectiveness reached 102.4%. Lee and Lee (2013) added porous coating on the wet channels of a RIEC and achieved wet-bulb effectiveness of 120%.

Despite the above-mentioned efforts, the broader application of IEC is still hindered by several intrinsic limitations. Firstly, the supply air temperature is restricted by the dew-point of the outdoor air, and the desired temperature cannot be reached when outdoor air is hot and humid (Chen et al., 2016). Secondly, IEC can only handle the sensible load and has little dehumidification capability. Thirdly, IEC consumes a certain amount of water as the driving force of cooling. Due to these limitations, IEC is not suitable for the GCC region, which has severe water scarcity and high ambient humidity.

To overcome the intrinsic limitations of IEC, several authors have proposed the hybridization of IEC and MVC (Chen et al., 2021). As shown in Fig. 1, the IEC and MVC are connected in tandem. The outdoor air is firstly pre-cooled in the IEC and then further processed in the MVC to achieve the desired temperature and humidity. Such a hybrid configuration can effectively control air temperature and humidity while sustaining a high energy efficiency. Moreover, the room return air can be used in the wet channels of IEC to recover the cold energy. Another advantage is that the condensate from the evaporator of MVC can be recovered to replenish the water consumption in IEC. With these promising features, IEC-MVC is suitable for cooling applications in most areas.

The hybrid IEC-MVC process has attracted substantial research interests. Cui et al. (2019a, 2015) studied the potential of the hybrid system in Singapore and found that IEC could handle 32% of the cooling load. Duan et al. (2019) studied the performance of IEC-MVC under the climatic conditions of Beijing and observed seasonal energy-saving of 38.2%. Chen et al. (2014) evaluated the potential of IEC-MVC in Hong Kong. The payback period was 2.9 years, and the cost-saving was 45% more than the enthalpy recovery wheel. Cui et al. (2019b) reported similar efforts for five cities: Xi'an, Athinai, Firenze, Cairo, and Singapore, and more than 35% of energy-saving potential was observed. Chen et al. (2017, 2015) developed an analytical model to evaluate the use of IEC as a pre-cooler of MVC. For similar purposes, Pandelidis et al. (2018) presented an ε-NTU-model, and Min et al. (2019b) developed a statistical model.

In our previous work (Chen et al., 2021), we presented a preliminary study on the hybrid IEC-MVC process. The IEC was operated as an enthalpy-recovery device to recover cold energy from the room exhaust air, and the effectiveness of enthalpy recovery was empirically correlated to the operating parameters. However, the energy-saving of the hybrid process was estimated analytically without experimental demonstration. Moreover, the previous study only focused on energy efficiency, and the water footprint has not been evaluated.

The current study is an extension of our previous work on the IEC-MVC process. A pilot IEC-MVC unit is fabricated and tested under different operating conditions (outdoor air temperature and humidity, air flowrate, compressor frequency), and the system is evaluated in terms of cooling performance, energy efficiency, and water consumption. Based on the experimental results, a simplified model is developed for rapid evaluation of the IEC-MVC process, and a case study is conducted under the climatic conditions of Saudi Arabia.

2. Methodology

A pilot IEC-MVC unit is commissioned by connecting the IEC unit presented in Chen et al. (2021) with an MVC cycle. Sensors are arranged at different locations to monitor the flowrate, temperature, and humidity of the air streams to monitor the system performance. Based on the measured parameters, the cooling performance, energy efficiency and water consumption of the hybrid system are evaluated.

2.1. Experimental design

The pilot IEC unit presented in our previous study (Chen et al., 2021) is connected with an MVC cycle to form the IEC-MVC process. The IEC consists of 100 dry and wet channels that are arranged in an alternating manner. The channels are separated by aluminum sheets with a thickness of 300 μm. Spray nozzles are installed at the entrance of the wet channels to supply water. Detailed information on the IEC is available in Chen et al. (2021).

The MVC unit consists of a compressor, an evaporator, a condenser, and a throttling valve. A commercial scroll compressor (Copeland™ ZR36K3E-TF5-522, Emerson) is selected, and its speed is regulated by a variable frequency drive (Altivar 320, Schneider). R134a is used as the refrigerant due to its broad applications. The evaporator and the condenser are fin-tube heat exchangers made of copper, and they are sized according to the design capacity.

The schematic of the hybrid IEC-MVC unit is shown in Fig. 2. The evaporator is placed after the exit of the dry channels, while the condenser is located after the wet channels. During operation, the outdoor air (1) firstly passes through the dry channels of the IEC to get pre-cooled. Then the pre-cooled air (2) is directed to the evaporator to be further processed to the desired temperature and humidity. The room return air (4) is used as the working fluid in the wet channels, where it contacts with the sprayed water to induce the evaporative cooling effect. After leaving the wet channels, the room exhaust air (5) is directed to the condenser to remove a portion of the condensation heat. The remaining

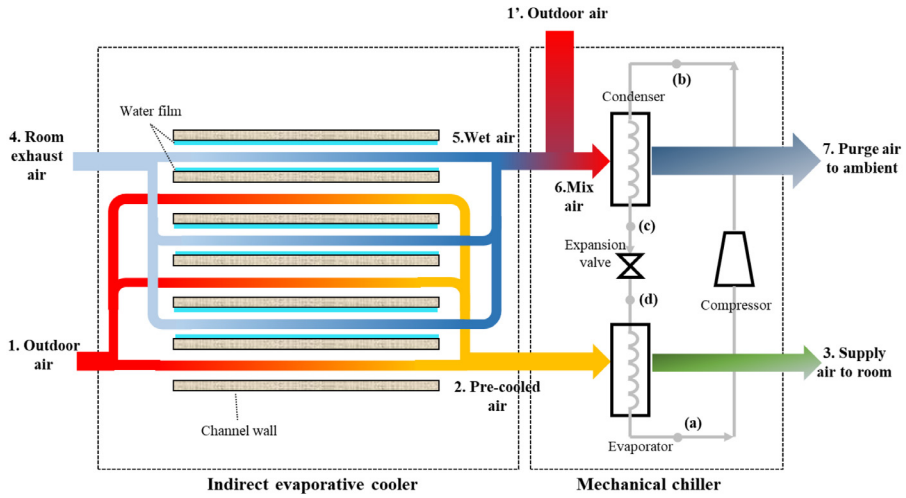

Fig. 1. Schematic of the hybrid IEC-MVC process (Chen et al., 2021).

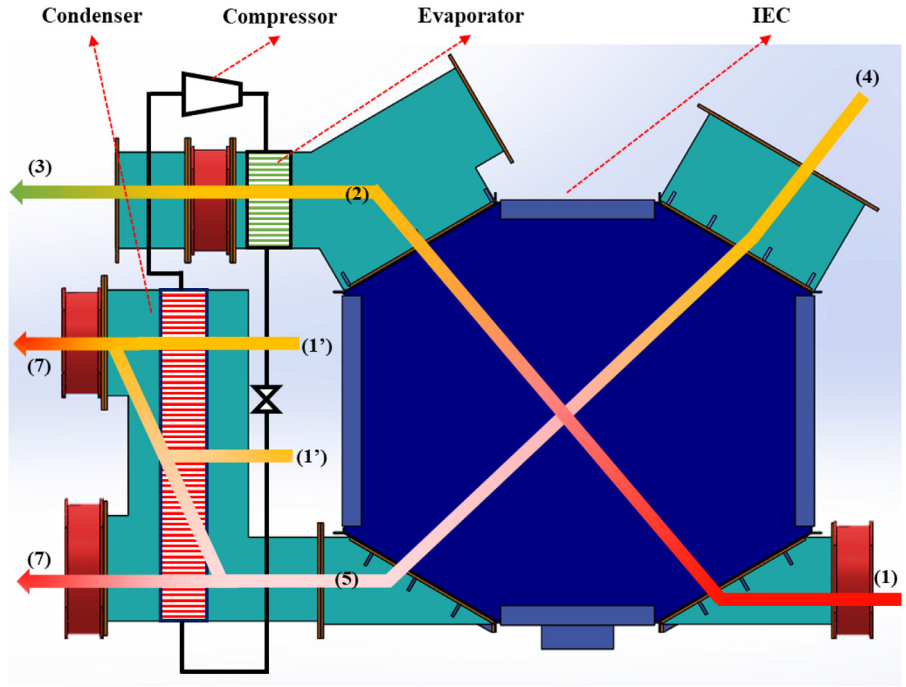

Fig. 2. KAUST proprietary design of the IEC-MVC unit, states 1–7 refer to the locations in Fig. 1.

condensation heat is removed using the outdoor air (1′) as the heat sink.

Fig. 3 shows the photo of the pilot IEC-MVC unit. The unit is housed inside an aluminum frame. To minimize heat loss, the surfaces are covered with insulation materials. Three containers are put below the unit to collect the condensate produced in the evaporator and the dry channels, which is mixed with the external water source (RO water at a temperature of ∼23 °C) and then supplied to the wet channels. The recovered condensate can reduce the water footprint of the process. Moreover, the condensate from the evaporator has the same temperature as the cold process air and will significantly promote the cooling performance of the IEC.

During experimental tests, the room air is supplied to the wet channels, while a mixture of the outdoor air and the room air is supplied to the dry channels to control the temperature and humidity. The air mixture is further heated with a 2000 W hot-air gun. The flowrates of the outdoor air and the return air are regulated by changing the fan speed. Temperature and humidity sensors are installed at different locations (1–6) to monitor the air conditions, and flow nozzles and differential pressure gauges are installed at the exits of the dry and wet channels to measure the air flowrates. The power consumption of the compressor, the fans, and the spray pump are measured and recorded using digital power meters. The technical specifications of the sensors are summarized in Table 1.

2.2. Performance indicators

Based on the measured parameters, the energy efficiency of the hybrid process, expressed as the coefficient of performance (COP), can be calculated. The COP is defined as the ratio of the cooling capacity to the energy input. For IEC, the COP is expressed as

$$COP_{IEC} = \frac{\dot{Q}_{IEC}}{P_{IEC}} = \frac{\dot{m}_{oa}(h_1 - h_2)}{P_{pump} + P_{fan,IEC}} \quad (1)$$

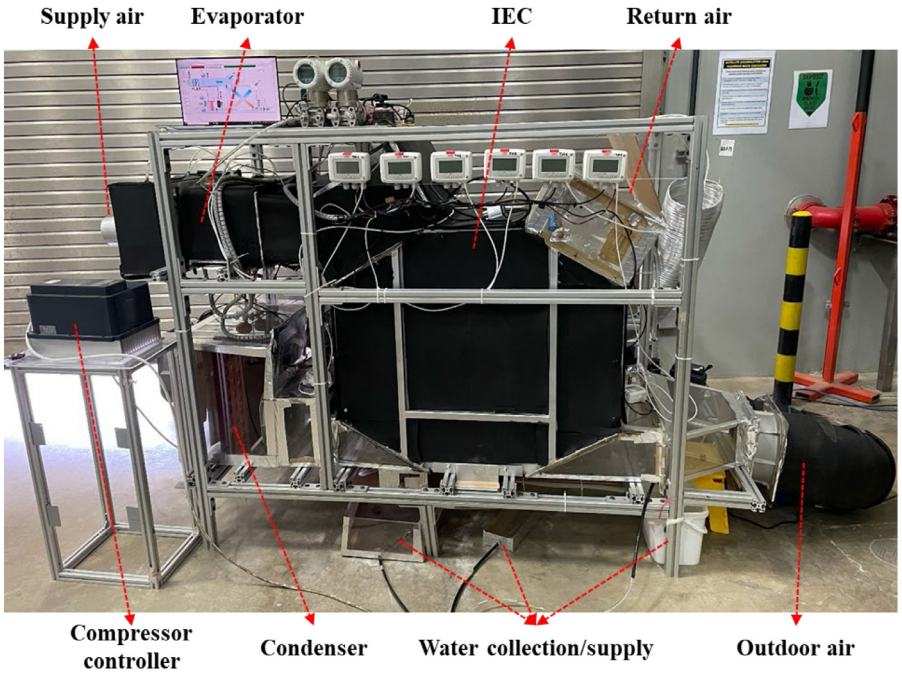

Fig. 3. Pilot IEC-MVC unit at KAUST.

Table 1
Technical data of measurement instrumentations.

Parameter	Sensor	Range	Accuracy
Temperature	TJ36-44004-1/8-12, OMIGA	0–60 °C	±0.1 °C
Relative humidity	FH400, Degree Controls Inc.	10%–90%	±2%
Pressure drop	2600T Series Pressure Transmitter, ABB	0–400 Pa	±5 Pa
Electrical power	PowerLogic PM5100, SCHNEIDER ELECTRIC	–	±0.5%

where $\dot{Q}_{IEC}$ and P_{IEC} represent the cooling capacity and power consumption, respectively. $\dot{m}_{oa}$ is the air flowrate in the dry channels, and h is the enthalpy of air. P_{pump} is the power consumption of the spray pump, and $P_{fan,IEC}$ is the overall electrical power of IEC fans.

Similarly, the COP of MVC and IEC-MVC can be calculated as

$$COP_{MVC} = \frac{\dot{Q}_{MVC}}{P_{MVC}} = \frac{\dot{m}_{oa}(h_2 - h_3)}{P_{comp} + P_{fan,IEC}} \tag{2}$$

$$COP_{IEC-MVC} = \frac{\dot{Q}_{total}}{P_{total}} = \frac{\dot{m}_{oa}(h_1 - h_3)}{P_{comp} + P_{pump} + P_{fan,IEC} + P_{fan,MVC}} \tag{3}$$

where P_{comp} is the compressor power, and $P_{fan,MVC}$ represents the power of the condenser fans.

In addition to the COP, the amount of cooling load handled by the IEC and the corresponding energy-saving are also important. The cooling capacity handled by IEC is computed as

$$\varnothing_{IEC} = \frac{\dot{Q}_{IEC}}{\dot{Q}_{total}} = \frac{\dot{m}_{oa}(h_1 - h_2)}{\dot{m}_{oa}(h_1 - h_3)} \tag{4}$$

And the energy-saving potential of the hybrid process over standalone MVC is derived as

$$\Delta COP = \frac{COP_{IEC-MVC} - COP_{MVC}}{COP_{IEC-MVC}} \tag{5}$$

One important difference between the proposed IEC-MVC process and standalone MVC (air-cooled) is that a certain amount of water is consumed in the IEC wet channels. Therefore, the amount of water consumption is also of great importance. The water consumption can be calculated from the change of moisture content in the wet channels

$$\dot{m}_{IEC} = \dot{m}_{ra}(\omega_5 - \omega_4) \tag{6}$$

Part of the water supply comes from the condensate collected from the supply air

$$\dot{m}_{cond} = \dot{m}_{oa}(\omega_1 - \omega_3) \tag{7}$$

Therefore, the net water consumption is expressed as

$$\dot{m}_{net} = \dot{m}_{IEC} - \dot{m}_{cond} \tag{8}$$

3. Results and discussion

This section presents the performance of the hybrid IEC-MVC process. The supply air conditions (temperature and humidity), energy efficiency, and water consumption are firstly evaluated under different conditions. Afterward, the energy-saving potential of the proposed IEC-MVC process over standalone MVC is discussed. Based on the derived results, a simplified model is developed for rapid prediction of IEC-MVC performance, and a case study is presented under the weather conditions of Saudi Arabia.

3.1. Cooling performance

The pilot IEC-MVC unit is tested under different outdoor air conditions (temperature, humidity ratio, and flowrate) and compressor speeds. As the air supplied to the dry channels is a mixture of the outdoor air and the room air, the temperature and humidity ratio are in the range of 30–40 °C and 10–20 g/kg, respectively. The air flowrate in the dry channels is regulated between 250–460 CMH, and the wet channel air flowrate is set to be close to the dry channel flowrate. This is because room exhaust air is used as the working air in the wet channels, and the available amount is almost the same as the outdoor air

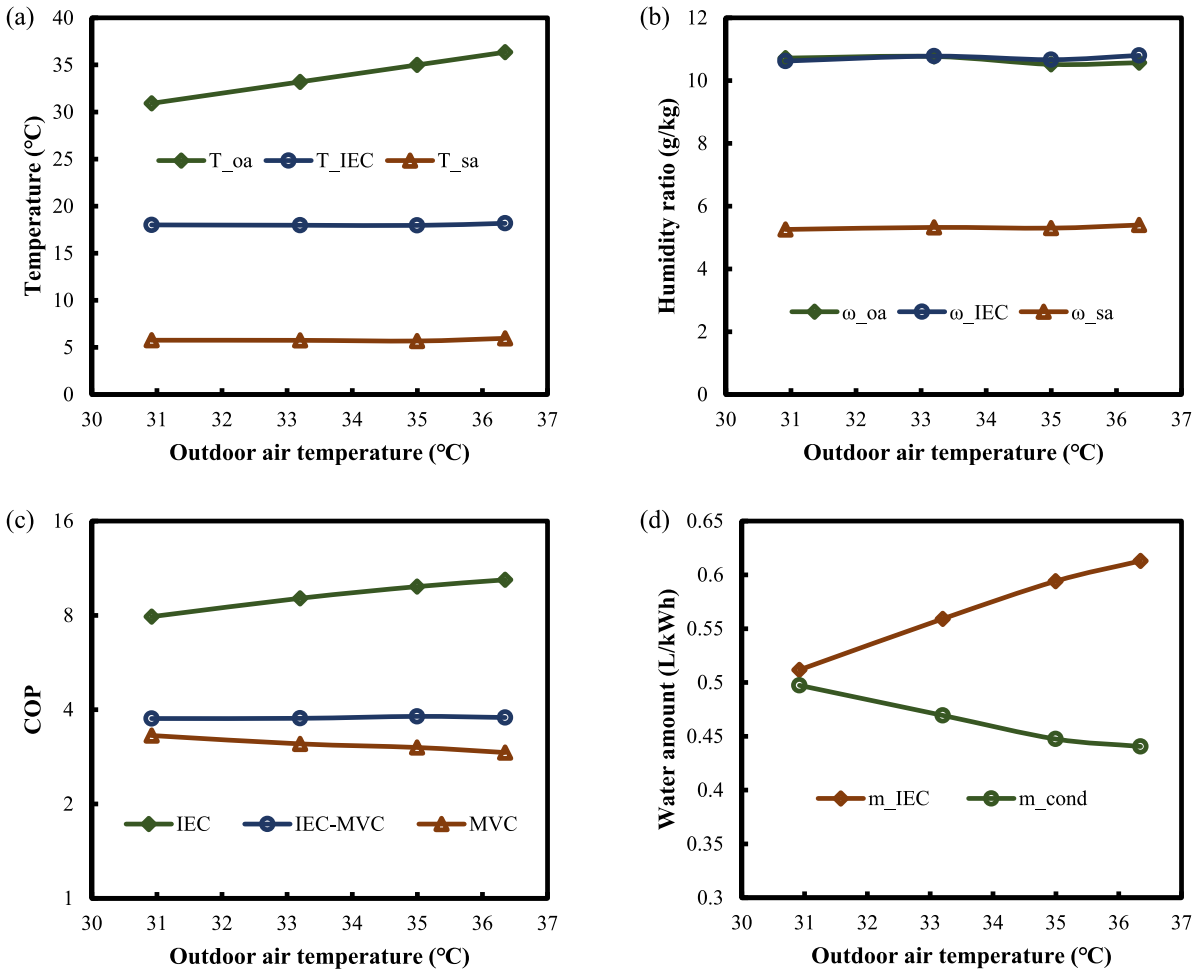

Fig. 4. Effect of outdoor air temperature on (a) outlet temperatures, (b) humidity ratio, (c) energy efficiency, and (d) water consumption. Outdoor humidity ratio = 10.6 g/kg, outdoor air flowrate = 300 CMH, and compressor frequency = 20 Hz.

Table 2
Parameter setting during experimental tests.

Parameter	Value/range
Outdoor air temperature (°C)	30–40
Outdoor air humidity ratio (g/kg)	10–20
Air flowrate (CMH)	250–460
Compressor frequency (Hz)	20–50

intake. Finally, the compressor frequency ranges 20–50 Hz. The parameter setting is summarized in Table 2.

Fig. 4 presents the system performance under different outdoor air temperatures with a fixed outdoor humidity ratio of 10.6 g/kg. As shown in Fig. 4(a), the IEC always cools the air to ∼18 °C, regardless of the outdoor air temperature. Such an observation differs from a regular IEC, whose outlet temperature increases with the increase of inlet temperature (Chen et al., 2020). The reason can be explained as follows. Firstly, the working air flowrate in the wet channels of our system is close to that in the dry channels. This differs from a regular IEC, where the wet channel flowrate is only 35%–50% of the dry channel flowrate. A higher working air flowrate induces more evaporative potential. Secondly, the cold condensate from the evaporator, which has the same temperature as the off-coil air (∼6 °C), is recovered and supplied to the wet channels to enhance the cooling effect. Moreover, the outdoor air has low humidity and requires only sensible cooling. Therefore, IEC is able to cool down the outdoor air to a similar temperature under different outdoor temperatures. After the IEC, the evaporator coils further cool down the air to 6 °C.

Fig. 4(b) shows the change in air humidity ratio. Similar to most IECs, the humidity ratio remains constant along the dry channels, as the air temperature is higher than its dew point temperature. After leaving the IEC, the air is dehumidified to 5 g/kg in the evaporator coils. The processed air (6 °C and 5 g/kg) can be mixed with the return air to achieve room thermal comfort.

Fig. 4(c) plots the COP of IEC, MVC, and IEC-MVC under different outdoor air temperatures. With the increase of the outdoor air temperature, the COP of IEC increases linearly due to more evaporative cooling potential. On the other hand, the COP of MVC decreases with increasing outdoor air temperature, because the compressor has to compress the refrigerant to a higher pressure for heat rejection. The conflicting effects of temperature on IEC and MVC offset each other in the hybrid process, leading to little change in hybrid COP.

The amounts of water consumption by IEC and condensate collection from the evaporator are plotted in Fig. 4(d). The values are normalized with respect to the total cooling capacity. As shown in the figure, the water consumption in the wet channels is linearly proportional to the outdoor temperature, as the evaporation of water is the main driving force for IEC cooling. On the other hand, the amount of condensate per kWh of cooling capacity decreases with increasing temperature. This is because the net amount of water collected remains the same (the evaporator always dehumidifies the outdoor air to 5 g/kg), while the cooling capacity

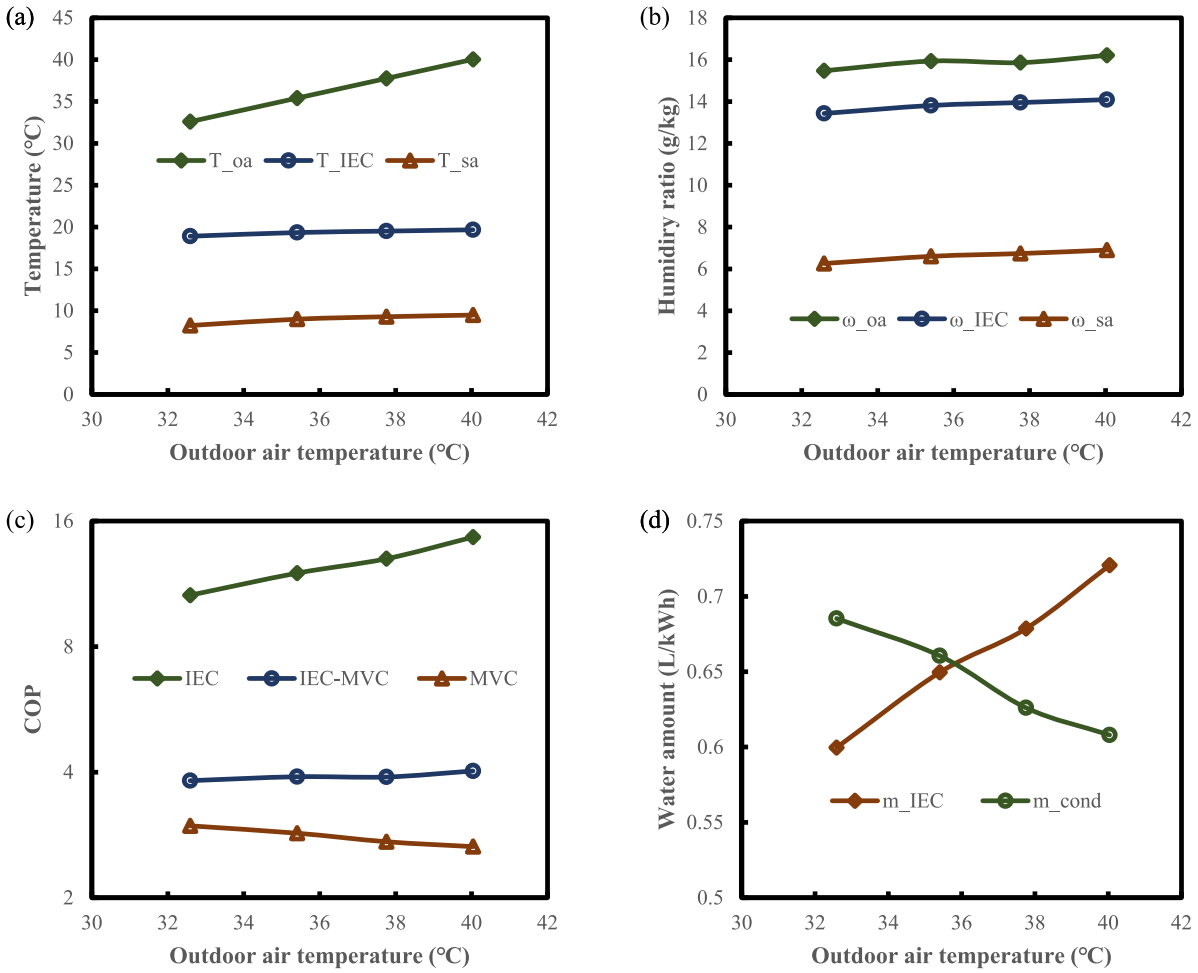

Fig. 5. Effect of outdoor air temperature on (a) outlet temperatures, (b) humidity ratio, (c) energy efficiency, and (d) water consumption. Outdoor humidity ratio = 16 g/kg, outdoor air flowrate = 300 CMH, and compressor frequency = 20 Hz.

gets higher. The collected condensate can provide 72%–95% of the water consumption in IEC, and the need for external water supply is marginal at 0.01–0.17 L per kWh of cooling effect. The net water consumption is much lower than that of a regular IEC (2–4 L/kWh under the weather condition of GCC countries (Baakeem et al., 2019)), making the hybrid IEC-MVC applicable in arid areas that have limited access to fresh water.

When the outdoor air humidity is high at 16 g/kg, the total cooling load increases, and the system shows a different response to temperature change. Compared with the low-humidity case, the air temperatures leaving IEC and MVC increase slightly with the increase in outdoor temperature, as revealed in Fig. 5(a). Another major difference is that there is a drop in air humidity along the IEC dry channels, as shown in Fig. 5(b). This is because the dew point temperature of the air is higher than the dry-bulb temperature in the dry channels.

Due to more drops of air enthalpy in the dry channels, the COP of IEC is higher at 10.5–14.5, as compared to 8–10 in the previous case. The overall trend of COP change remains the same, i.e., a higher outdoor temperature promotes the COP of IEC while reducing the COP of MVC, and the hybrid COP remains constant.

With higher humidity, more condensate can be collected from the outdoor air, as can be seen in Fig. 5(d). The condensation rate is 0.6–0.7 L/kWh in the present case, while the amount is lower at 0.4–0.5 L/kWh when the humidity ratio is 10.6 g/kg. The collected condensate is sufficient for the wet channels when the IEC cooling load is not too high, i.e., $T_{oa} < 36$ °C, and the excess condensate can be used somewhere else.

Fig. 6 presents the system's response to the compressor frequency. With a higher compressor frequency, a lower evaporator temperature can be achieved. As a result, the air leaving the coils has a lower temperature and humidity, as can be seen in Fig. 6(a) and (b). The COP of MVC drops with compressor frequency, as plotted in Fig. 6(c). This is attributed to a higher compression ratio, which leads to more compression power. Finally, more condensate can be collected from the outdoor air due to a higher level of dehumidification, as shown in Fig. 6(d).

The compressor frequency also has an impact on the performance of IEC. Under a higher compressor frequency, the condensate temperature is significantly reduced, as it follows the process air temperature. As a result, the performance of IEC is promoted. The air temperature and humidity are lower when leaving the IEC, leading to a higher COP. However, the hybrid COP shows a decreasing trend, as it is dominated by the MVC performance.

Fig. 7 shows the system performance under different air flowrates. Due to a limited heater capacity, the inlet temperature drops with the flowrate. However, the air temperature and humidity are still higher when leaving the IEC (shown in Fig. 7(a–b)), which is a result of a limited heat transfer area and a shorter contact time. For the same reason, the off-coil temperature and humidity ratio also increase with the flowrate, and the variations are more significant. Under the flowrate range considered, the supply air temperature and humidity ratio are varied by 7 °C and 3.5 g/kg, respectively. During practical operation, the flowrate can be an addition to the compressor frequency for controlling supply air condition and cooling load.

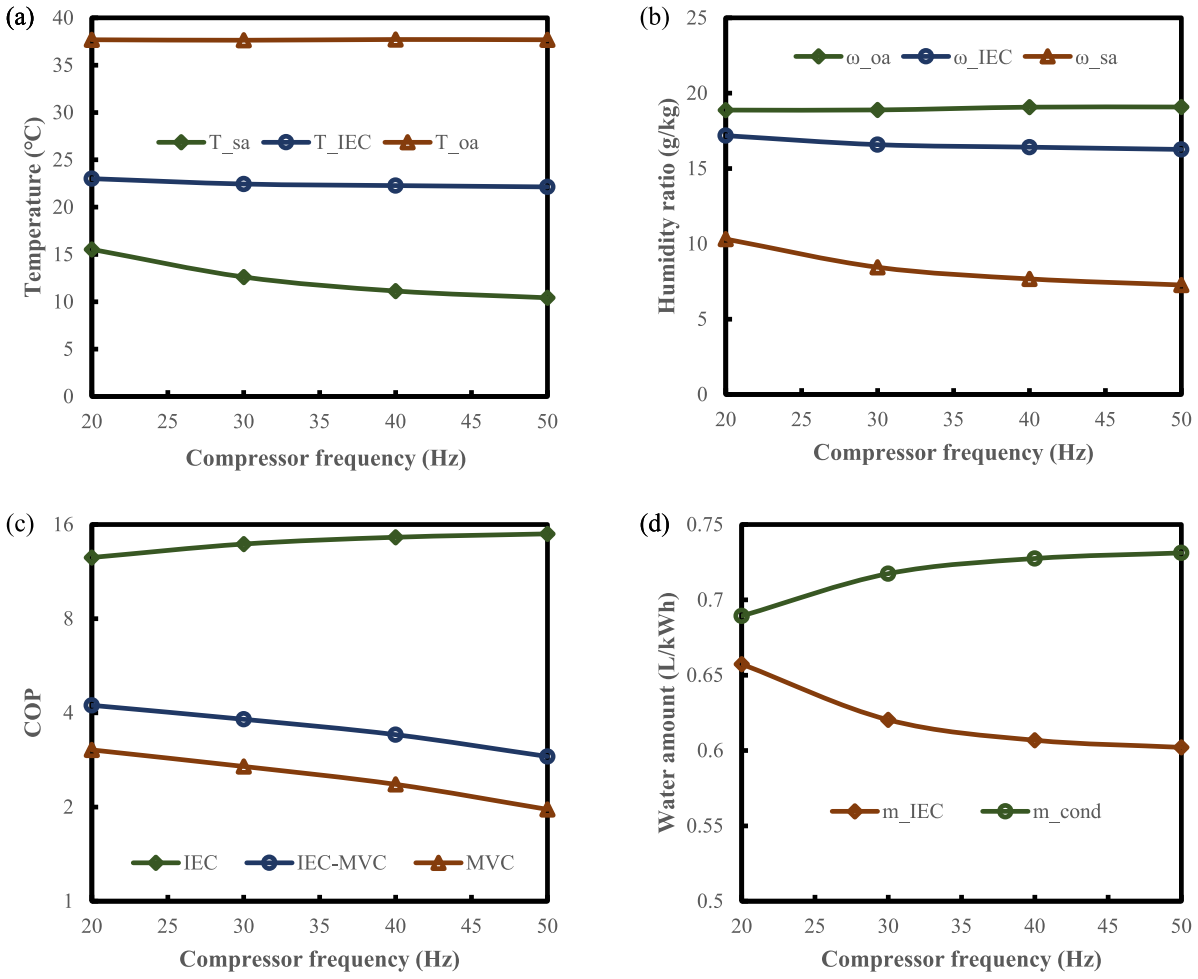

Fig. 6. Effect of compressor frequency on (a) outlet temperatures, (b) humidity ratio, (c) energy efficiency, and (d) water consumption. Outdoor temperature = 38 °C, outdoor humidity ratio = 19 g/kg, and outdoor air flowrate = 350 CMH.

With a smaller temperature drop and a higher fan power, the COP of IEC drops with flowrate, as presented in Fig. 7(c). However, the COP for MVC and the hybrid IEC-MVC process demonstrate a reverse trend, which is attributed to a higher evaporator temperature that lowers the compressor power. A higher air flowrate also introduces more moisture content into the system and leads to more condensation, as plotted in Fig. 7(d). On the other hand, the water consumption of IEC firstly declines, and the trend is reversed after the flowrates exceed 400 CMH. The inflection point can be attributed to the increase of IEC cooling load. When the flowrate increases from 250 to 400 CMH, the temperature and humidity difference between the inlet and outlet becomes smaller, and the total cooling load (the product of the air flowrate and the enthalpy difference) shows a decreasing trend. However, when the air flowrate increases from 400 to 450 CMH, the drop of air enthalpy change is less significant, and the total cooling load starts to increase.

3.2. Energy saving potential

From the above results, it can be seen that the hybrid IEC-MVC process benefits from the high energy efficiency of IEC and has a higher COP than standalone MVC. The COP improvement is directly related to the percentage of cooling capacity contributed by IEC, as summarized in Fig. 8. According to Fig. 8(a–b), IEC handles a higher portion of cooling load when the outdoor temperature and humidity are higher, and the corresponding improvement of COP over MVC is also more obvious. Under a dry ambient condition, IEC handles up to 40% of the cooling load, and the hybrid COP is 22% higher than that of MVC. When the outdoor air is humid, the cooling capacity contributed by IEC can achieve 50%, leading to a 34% increase in COP.

A higher compressor speed also promotes IEC cooling capacity, which is caused by the supply of colder condensate to the wet channels. Consequently, the cooling capacity of IEC gets higher, and the improvement of COP is more significant, as shown in Fig. 8(c). When the compressor frequency increases from 20 to 50 Hz, the cooling load of IEC is increased from 32% to 39%, and the improvement of COP is varied from 28% to 32%.

Fig. 8 (d) shows the COP improvement under different air flowrates. The numbers seem to be marginally impacted by the air flowrate. However, this is partially due to a reduced outdoor air temperature under a higher air flowrate, and it does not represent the intrinsic behavior of the system. If a constant outdoor air temperature is considered, more COP improvement can be expected under a higher air flowrate.

3.3. Empirical model

Based on the derived results, we develop a simplified model that allows for a rapid evaluation of the IEC-MVC performance. The model firstly calculates the cooling capacity and energy efficiency of the IEC, then predicts the MVC performance, and finally analyzes the hybrid IEC-MVC process.

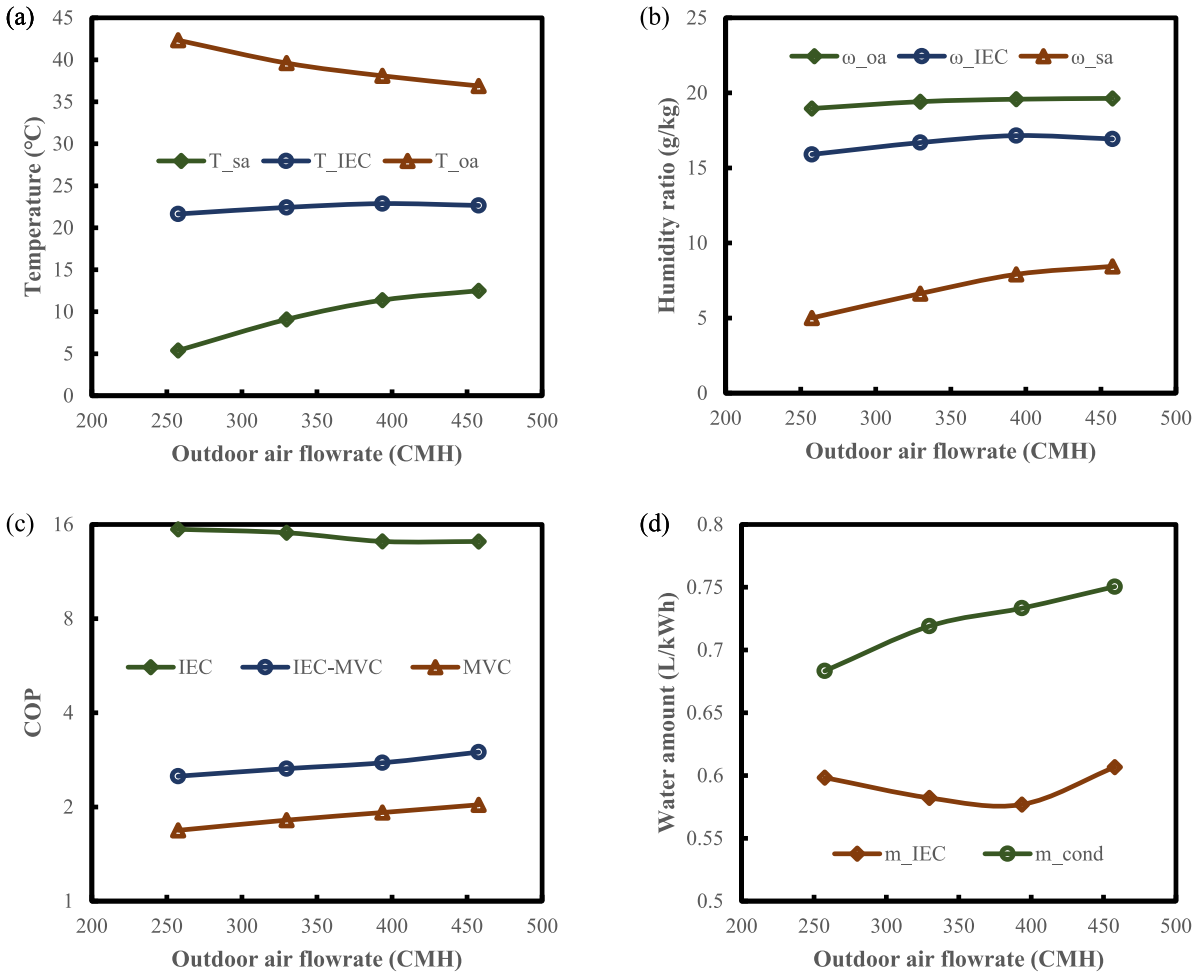

Fig. 7. Effect of outdoor air flowrate on (a) outlet temperatures, (b) humidity ratio, (c) energy efficiency, and (d) water consumption. Outdoor temperature = 38 °C, outdoor humidity ratio = 19 g/kg, and compressor frequency = 50 Hz.

The cooling capacity of IEC can be calculated from the enthalpy effectiveness, which is defined as (Chen et al., 2021)

$$\varepsilon = \min\{\frac{h_1 - h_2}{h_1 - h_{2,s}}, \frac{h_5 - h_4}{h_{5,s} - h_4}\} \tag{9}$$

where $h_{2,s}$ and $h_{5,s}$ represent the maximum/minimum enthalpy that the air streams can achieve, i.e., the outdoor air reaches the temperature of the room air when leaving the dry channels, and the room exhaust air in the wet channels has the same temperature as the incoming outdoor air.

According to our previous study, the effectiveness of IEC is determined by the temperature, humidity, and flowrate of the air streams (Chen et al., 2021). The correlation is provided in Eq. (10) and its discrepancy with the measurement is within 3.5%.

$$\varepsilon = 0.416 - 5.81 \times 10^{-3} T_{oa} + 4.65 \times 10^{-3} \omega_{oa} + 1.42 \times 10^{-3} T_{ra} - 5.65 \times 10^{-3} \omega_{ra} + 7.49 \times 10^{-4} \frac{\dot{m}_{oa}}{\dot{m}_{ra}} \tag{10}$$

Eqs. (9) and (10) determine the change of air enthalpy in IEC, based on which the energy efficiency can be achieved. Fig. 9(a) shows the relationship between the enthalpy change and the COP. It is obvious that the COP of IEC is a linear function of the enthalpy change, which is expressed as

$$COP_{IEC} = 0.4892 \times \Delta h + 1.4254 \tag{11}$$

The coefficient of determination (R^2) is 0.9877, and the maximum deviation is 3.7%.

The energy efficiency of air-cooled MVC is determined by the temperature difference between the evaporator and the condenser, as plotted in Fig. 9(b). The relationship is quantified in Eq. (12) with a maximum deviation of 3.1%.

$$COP_{MVC} = 0.0304 \times T_{sa} - 0.0761 \times T_{oa} + 4.992 \tag{12}$$

Employing the above equations, the performance of the IEC-MVC process can be easily estimated. Based on the temperature, humidity ratio, and flowrate of the outdoor air and room air, the cooling load, power consumption, and water consumption in the IEC can be calculated through Eqs. (9)–(11) and Eq. (6). Afterward, the supply air temperature and humidity can be determined by the total cooling load, based on which the energy consumption of MVC and the water footprint can be calculated using Eqs. (7)–(8) and Eq. (12). The process is schematically demonstrated in Fig. 10.

3.4. Case study in Saudi Arabia

Employing the simplified model, we estimate the annual energy-saving potential of IEC-MVC in the main cities of Saudi Arabia. 13 cities from different provinces are selected and their annual weather data (temperature and relative humidity) with an hourly resolution are acquired from Meteomatics Weather API (Meteomatics Weather, API, 2022). To quantify the need for cooling and dehumidification, we introduce two parameters, namely, cooling degree hours (CDH) and dehumidifying gram

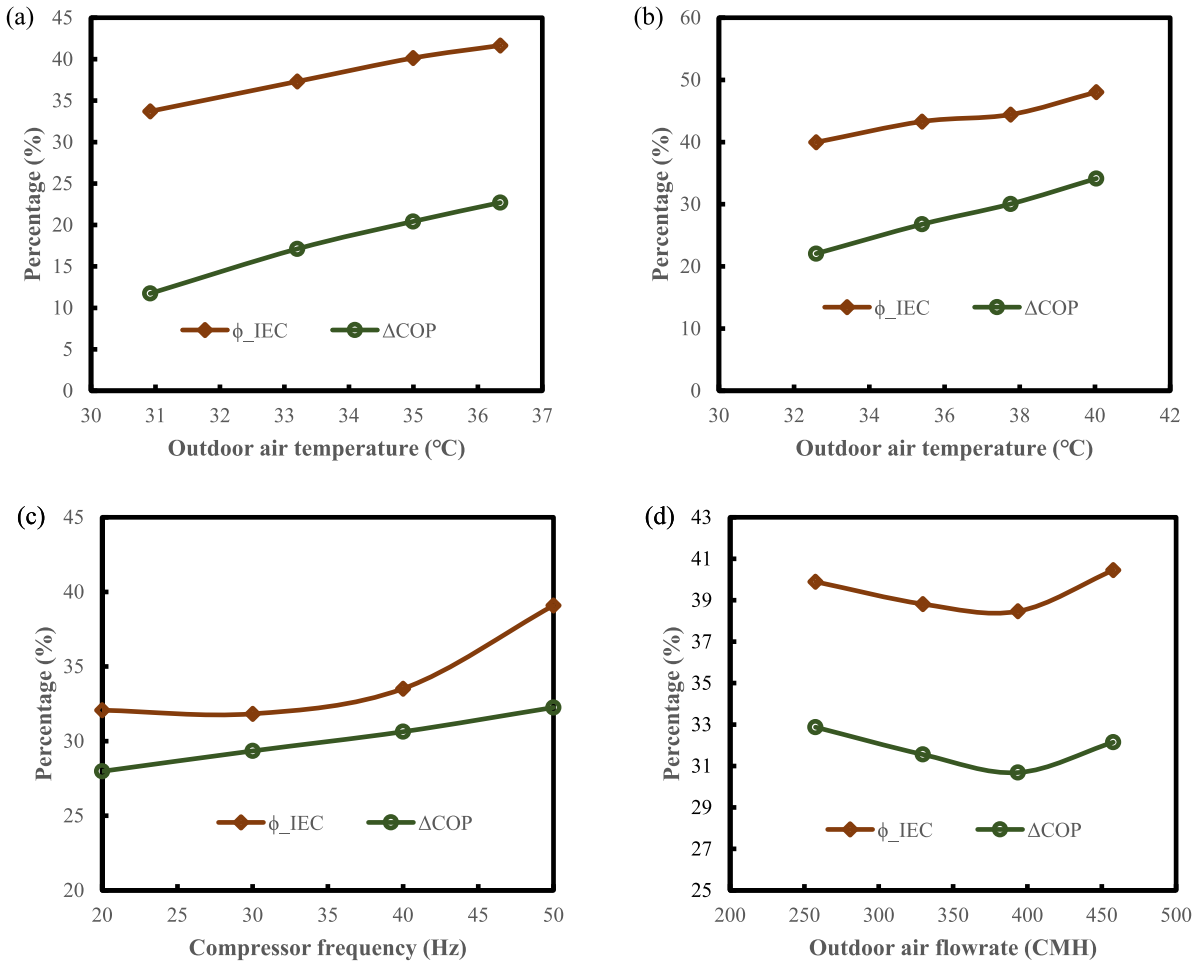

Fig. 8. Energy-saving potential of IEC-MVC under different (a–b) outdoor air temperatures: (a) outdoor humidity ratio = 11 g/kg and (b) outdoor humidity ratio = 16 g/kg, (c) compressor frequency, and (d) outdoor air flowrate.

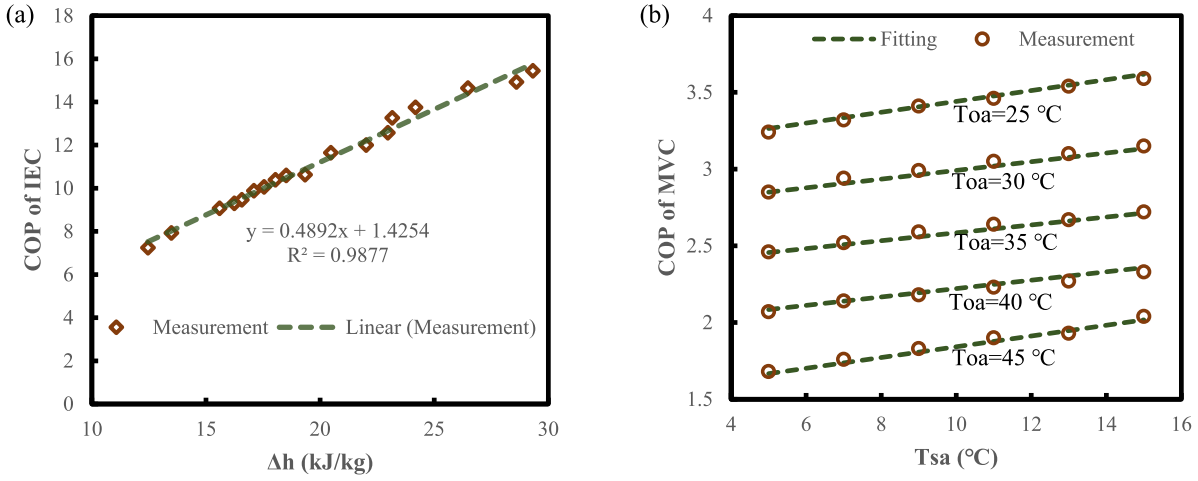

Fig. 9. Comparison of measured COP with derived correlation for (a) IEC and (b) MVC.

hours (DGM). CDH is similar to the concept of cooling degree days (CDD) but calculated on an hourly basis:

$$CDH = \sum (T - 18\ ^{\circ}\mathrm{C})\ when\ T > 18\ ^{\circ}\mathrm{C} \tag{13}$$

where T is the hourly average temperature in °C. CDH quantifies the amount of cooling demand and its duration. Similarly, DGM is a measurement of dehumidification demand in g/kg and its duration:

$$DGH = \sum (\omega - 9\ \mathrm{g/kg})\ when\ \omega > 9\ \mathrm{g/kg} \tag{14}$$

where ω is the hourly average humidity ratio of the ambient air.

The CDH and DGM for 13 representative cities of Saudi Arabia are summarized in the 4th and 5th columns of Table 3. Most cities have high cooling demand, as quantified by high values of

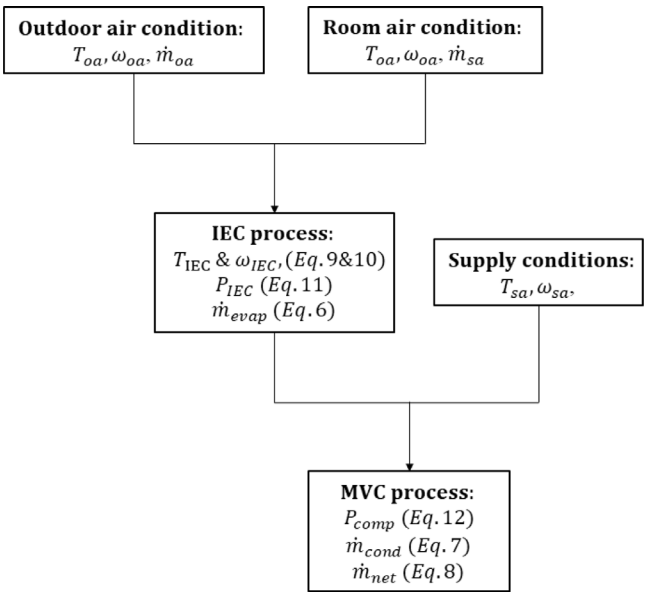

Fig. 10. Rapid estimation of IEC-MVC performance.

CDH. Jazan has the maximum CDH of 111 837 °C-h, indicating an average cooling demand of 12.7 °C over the whole year (8760 h). The CDH for Riyadh, Qassim, Dhahran, Makkah and Madinah also exceed 80 000 °C-h. Abha and Al-Bahah, in contrast, have little cooling demand due to a high latitude of >2000 m. In addition to the sensible cooling demand, certain cities also need dehumidification due to high ambient humidity. These cities include Dhahran (DGH = 22 225 g-h/kg), Makkah (DGH = 22 225 g-h/kg) and Jazan (DGH = 58 262 g-h/kg).

Columns 6–7 in Table 3 show the contributions of IEC and the energy-saving over standalone MVC. The proposed system shows excellent performance in hot and dry cities, i.e. Riyadh, Hail, Qassim, Al-Jouf, Turaif, Tabuk, Madinah and Najran. In these cities, IEC can handle >50% of the total cooling load, leading to 40%–60% of energy savings. In hot and humid cities (Dhahran, Mecca and Jazan), the performance degrades slightly, but there is still ∼20% of energy saving.

The last two columns summarize the water footprint. The water consumption of IEC is in the range of 6–20 L/h for 1 kg/s of outdoor air, depending on the cooling load of IEC. Such water consumption can be compensated by the condensate collected in the MVC evaporator. For example, the collected condensate can account for 46% and 58% of the water consumption in Makkah and Dhahran, respectively. In Jazan, the amount of condensate is more than the water consumption, and the excess water can be used elsewhere.

4. Conclusions

A pilot IEC-MVC unit is fabricated and tested under different conditions to evaluate its performance, including the capability of temperature and humidity control, the energy-saving potential over MVC, and the water footprint. The following concluding remarks can be derived from the results:

(1) The IEC can pre-cool the outdoor air to ∼20 °C by recovering cold energy from the room exhaust air. When the outdoor humidity is high, IEC also dehumidifies the outdoor air by 1–2 g/kg;
(2) The pre-cooled air can be further processed to 5–15 °C and 5–10 g/kg by MVC. The supply air temperature and humidity can be regulated by changing the compressor frequency and the air flowrate;
(3) The IEC handles 35%–50% of the total cooling load, and the energy consumption of the hybrid process is 15%–35% lower than standalone MVC;
(4) The recovered condensate can compensate for >70% of water consumption in IEC. When the outdoor humidity is high, the system produces excess freshwater;
(5) The proposed process is suitable for most cities in Saudi Arabia. The energy-saving potential of the system is higher in hot and dry regions, while the water footprint is smaller in humid areas.

Nomenclature

Abbreviations

AC	Air conditioning
CDD	Cooling degree days
CDH	Cooling degree hours
COP	Coefficient of performance
DGH	Dehumidifying gram hours
IEC	Indirect evaporative cooler
MVC	Mechanical vapor compression

Symbols

h	Specific enthalpy, J/kg
m	Mass flowrate, kg/s
P	Electricity consumption, W
Q	Cooling load, W
T	Temperature, °C
X	Cooling load ratio, %

Greek letters

ε	Effectiveness, %
ϕ	Percentage of cooling load handled by IEC, %
ω	Humidity ratio, g/kg

Subscripts

comp	Compressor
cond	Condensation
evap	Evaporation
fan	Fan
ma	Mixed air
net	Net water consumption
oa	Outdoor air
pump	Pump
ra	Room exhaust air
s	Saturated
sa	Supply air
total	Total

CRediT authorship contribution statement

Qian Chen: Conceptualization, Methodology, Formal analysis, Writing – original draft. **M. Kum Ja:** Methodology, Software, Validation, Investigation. **Muhammad Burhan:** Validation, Formal analysis. **Muhammad Wakil Shahzad:** Formal analysis. **Doskhan Ybyraiymkul:** Formal analysis. **Hongfei Zheng:** Formal analysis. **Kim Choon Ng:** Writing – review & editing, Supervision, Project administration, Funding acquisition.

Declaration of competing interest

The authors declare that they have no known competing financial interests or personal relationships that could have appeared to influence the work reported in this paper.

Table 3
Long-term performance of IEC-MVC in different cities of Saudi Arabia.

Region	Province	Representative city	CDH, °C-h/year	DGH, g-h/year	ϕ_IEC,%	Energy saving, %	Water consumption, L/h	Water collection, L/h
Middle	Ar-Riyadh	Riyadh	92 248.4	432.57	54.35	40.52	8.57	0.18
	Hail	Hail	71 265.4	6.84	53.65	37.57	6.33	0.00
	Al-Qassim	Qassim	88 722.4	124.65	54.96	40.98	8.21	0.04
East	Eastern Region	Dhahran	89 967.1	22 225.80	31.27	26.04	9.15	8.25
	Al-Jouf	Al-Jouf	65 980.4	9.24	53.71	37.83	5.87	0.00
	Northern Borders	Turaif	48 481.6	86.82	50.14	33.44	3.94	0.01
West	Tabuk	Tabuk	62 562.6	155.29	51.94	36.12	5.36	0.03
	Makkah	Mecca	107 079.7	21 044.16	32.77	24.78	10.86	7.90
	Al-Madinah	Madinah	101 092.6	995.84	53.49	40.15	9.53	0.25
South	Aseer	Abha	17 674.9	815.62	15.32	7.55	0.38	0.01
	Jazan	Jazan	111 837.0	58 262.63	22.39	17.20	12.22	23.56
	Najran	Najran	58 329.4	409.75	45.09	28.13	4.29	0.11
	Al-Bahah	Al-Bahah	20 167.7	1113.43	15.46	7.87	0.51	0.04

Acknowledgment

This research was supported by the Water Desalination and Reuse Center, Biological and Environmental Science and Engineering Division, King Abdullah University of Science and Technology.

References

Ali, M., Ahmad, W., Sheikh, N.A., Ali, H., Kousar, R., ur Rashid, T., 2021. Performance enhancement of a cross flow dew point indirect evaporative cooler with circular finned channel geometry. J. Build. Eng. 35, 101980.

Baakeem, S.S., Orfi, A., Mohamad, J., Bawazeer, S., 2019. The possibility of using a novel dew point air cooling system (M-Cycle) for A/C application in Arab Gulf countries. Build. Environ. 148, 185–197.

Boukhanouf, R., Alharbi, A., Ibrahim, H.G., Amer, O., Worall, M., 2017. Computer modelling and experimental investigation of building integrated sub-wet bulb temperature evaporative cooling system. Appl. Therm. Eng. 115, 201–211.

Boukhanouf, R., Amer, O., Ibrahim, H., Calautit, J., 2018. Design and performance analysis of a regenerative evaporative cooler for cooling of buildings in arid climates. Build. Environ. 142, 1–10.

Chen, Q., Burhan, M., Shahzad, M.W., Ybyraiymkul, D., Akhtar, F.H., Ng, K.C., 2020. Simultaneous production of cooling and freshwater by an integrated indirect evaporative cooling and humidification-dehumidification desalination cycle. Energy Convers. Manage. 221, 113169.

Chen, Q., Ja, M.K., Burhan, M., Akhtar, F.H., Shahzad, M.W., Ybyraiymkul, D., Ng, K.C., 2021. A hybrid indirect evaporative cooling-mechanical vapor compression process for energy-efficient air conditioning. Energy Convers. Manage. 248, 114798.

Chen, Y., Luo, Y., Yang, H., 2014. Fresh air pre-cooling and energy recovery by using indirect evaporative cooling in hot and humid region–a case study in Hong Kong. Energy Procedia 61, 126–130.

Chen, Y., Luo, Y., Yang, H., 2015. A simplified analytical model for indirect evaporative cooling considering condensation from fresh air: Development and application. Energy Build. 108, 387–400.

Chen, Y., Yang, H., Luo, Y., 2016. Indirect evaporative cooler considering condensation from primary air: Model development and parameter analysis. Build. Environ. 95, 330–345.

Chen, Y., Yang, H., Luo, Y., 2017. Parameter sensitivity analysis and configuration optimization of indirect evaporative cooler (IEC) considering condensation. Appl. Energy 194, 440–453.

Cui, X., Chua, K., Ng, K.C., 2015. Performance evaluation of an indirect pre-cooling evaporative heat exchanger operating in hot and humid climate. Energy Convers. Manage. 102, 140–150.

Cui, X., Islam, M., Chua, K., 2019a. An experimental and analytical study of a hybrid air-conditioning system in buildings residing in tropics. Energy Build. 201, 216–226.

Cui, X., Sun, L., Zhang, S., Jin, L., 2019b. On the study of a hybrid indirect evaporative pre-cooling system for various climates. Energies 12 (23), 4419.

Duan, Z., Zhan, C., Zhang, X., Mustafa, M., Zhao, X., Alimohammadisagvand, B., Hasan, A., 2012. Indirect evaporative cooling: Past, present and future potentials. Renew. Sustain. Energy Rev. 16 (9), 6823–6850.

Duan, Z., Zhan, C., Zhao, X., Dong, X., 2016. Experimental study of a counter-flow regenerative evaporative cooler. Build. Environ. 104, 47–58.

Duan, Z., Zhao, X., Zhang, Q., 2019. Dynamic simulation of a hybrid dew point evaporative cooler and vapour compression refrigerated system for a building using EnergyPlus. J. Build. Eng. 21, 287–301.

Eveloy, V., Ayou, D.S., 2019. Sustainable district cooling systems: Status, challenges, and future opportunities, with emphasis on cooling-dominated regions. Energies 12 (2), 235.

IEA, 2021. Global Air Conditioner Stock, 1990-2050. IEA, Paris, https://www.iea.org/data-and-statistics/charts/global-air-conditioner-stock-1990-2050.

Jia, L., Liu, J., Wang, C., Cao, X., Zhang, Z., 2019. Study of the thermal performance of a novel dew point evaporative cooler. Appl. Therm. Eng. 160, 114069.

Jradi, M., Riffat, S., 2014. Experimental and numerical investigation of a dew-point cooling system for thermal comfort in buildings. Appl. Energy 132, 524–535.

Kabeel, A., Abdelgaied, M., 2016. Numerical and experimental investigation of a novel configuration of indirect evaporative cooler with internal baffles. Energy Convers. Manage. 126, 526–536.

Kabeel, A., Bassuoni, M., Abdelgaied, M., 2017. Experimental study of a novel integrated system of indirect evaporative cooler with internal baffles and evaporative condenser. Energy Convers. Manage. 138, 518–525.

Lee, J., Lee, D.-Y., 2013. Experimental study of a counter flow regenerative evaporative cooler with finned channels. Int. J. Heat Mass Transfer 65, 173–179.

Meteomatics Weather, API, 2022. https://www.meteomatics.com/en/weather-api/.

Min, Y., Chen, Y., Yang, H., 2019a. Numerical study on indirect evaporative coolers considering condensation: A thorough comparison between cross flow and counter flow. Int. J. Heat Mass Transfer 131, 472–486.

Min, Y., Chen, Y., Yang, H., 2019b. A statistical modeling approach on the performance prediction of indirect evaporative cooling energy recovery systems. Appl. Energy 255, 113832.

Moshari, S., Heidarinejad, G., 2017. Analytical estimation of pressure drop in indirect evaporative coolers for power reduction. Energy Build. 150, 149–162.

Oh, S.J., Shahzad, M.W., Burhan, M., Chun, W., Jon, C.K., KumJa, M., Ng, K.C., 2019. Approaches to energy efficiency in air conditioning: a comparative study on purge configurations for indirect evaporative cooling. Energy 168, 505–515.

Pandelidis, D., Cichoń, A., Pacak, A., Anisimov, S., Drąg, P., 2018. Counter-flow indirect evaporative cooler for heat recovery in the temperate climate. Energy 165, 877–894.

Pandelidis, D., Niemierka, E., Pacak, A., Jadwiszczak, P., Cichoń, A., Drąg, P., Worek, W., Cetin, S., 2020. Performance study of a novel dew point evaporative cooler in the climate of central europe using building simulation tools. Build. Environ. 181, 107101.

Park, J.-Y., Kim, B.-J., Yoon, S.-Y., Byon, Y.-S., Jeong, J.-W., 2019. Experimental analysis of dehumidification performance of an evaporative cooling-assisted internally cooled liquid desiccant dehumidifier. Appl. Energy 235, 177–185.

Rashidi, S., Kashefi, M.H., Kim, K.C., Samimi-Abianeh, O., 2019. Potentials of porous materials for energy management in heat exchangers–A comprehensive review. Appl. Energy 243, 206–232.

Riffat, S., Zhu, J., 2004. Mathematical model of indirect evaporative cooler using porous ceramic and heat pipe. Appl. Therm. Eng. 24 (4), 457–470.

Shahzad, M.W., Burhan, M., Ybyraiymkul, D., Oh, S.J., Ng, K.C., 2019. An improved indirect evaporative cooler experimental investigation. Appl. Energy 256, 113934.

Shahzad, M.W., Lin, J., Xu, B.B., Dala, L., Chen, Q., Burhan, M., Sultan, M., Worek, W., Ng, K.C., 2021. A spatiotemporal indirect evaporative cooler enabled by transiently interceding water mist. Energy 217, 119352.

Wang, F., Sun, T., Huang, X., Chen, Y., Yang, H., 2017. Experimental research on a novel porous ceramic tube type indirect evaporative cooler. Appl. Therm. Eng. 125, 1191–1199.

Yang, H., Shi, Y., Min, Y., 2021. Research development of indirect evaporative cooling technology: An updated review. Renew. Sustain. Energy Rev. 145, 111082.

Zhao, X., Liu, S., Riffat, S.B., 2008. Comparative study of heat and mass exchanging materials for indirect evaporative cooling systems. Build. Environ. 43 (11), 1902–1911.